И Н С Т И Т У Т
ЯДЕРНОЙ ФИЗИКИ СОАН СССР

ПРЕПРИНТ И Я Ф 76-121

L.M.Barkov, V.B.Baryshev, G.A.Blinov, E.N.Gubanov,
N.I.Krupin, N.M.Ryskulev, E.P.Solodov, B.I.Hazin,
V.M.Horev, V.N.Zaitsev

A CRYOGENIC MAGNETIC DETECTOR FOR VEPP-2M

Новосибирск
1976

A CRYOGENIC MAGNETIC DETECTOR FOR VEPP-2M

L.M.Barkov, V.B.Baryshev, G.A.Blinov, E.N.Gubanov,
N.I.Krupin, N.M.Ryskulov, E.P.Solodov, B.I.Hazin,
V.M.Horev, V.N.Zaitsev

Institute of Nuclear Physics
Siberian Division of the USSR Academy of Sciences

1. General Description

To study the reaction products from e^+e^- collisions at the storage ring facility VEPP-2M /1/ the cryogenic magnetic detector has been made. A schematic cross section of the detector is shown in Fig.1. The size of the VEPP-2M straight line section determines detector's proportions. The optical spark chamber (6) with six gaps is placed in the magnetic field that is created by superconducting solenoid (7). The solenoid and the spark chamber axes are parallel to the particle motion direction in the storage ring. The spark chamber operates in the track mode at temperature about 170-180 K and pressure about 2 atm. The high gas density allows to obtain rather good spatial resolution $\sigma_R \sim 55\mu$. The cylindrical multiwire proportional chambers (MWPC) (8, 9) are used for spark chamber to trigger. They operate at the same conditions as the spark chamber. The solid angle of the detector is $0.6 \times 4\pi$. Two compensating superconducting solenoids (5) with the opposite sign of the magnetic field are employed to reduce the influence of the main solenoid on particles motion in the storage ring.

2. Superconducting Solenoids

The magnetic set-up of the detector is scethed in Fig.2. It consists of three superconducting solenoids - the main one (8) and two compensating (9). The basic features of the solenoids are listed in Table 1.

Table 1

	main solenoid	compensating solenoids
1. The inner diameter of the coil, mm	323	36
2. The outer diameter of the coil, mm	404	62
3. The length of the coil, mm	320	153
4. The diameter of the cable, mm	1.5	0.7
5. Number of turns	4161	3040
6. The critical current of the coil, A	270	210
7. The magnetic field in the center of the solenoid at the critical current, kGs	33	50
8. The maximum working current when all solenoids are switched on together	220	160
9. The maximum working field in the center of the detector	27	-
10. The store energy, kdg	150	2

The solenoids have been wound with partially stabilized NbTi cable, which allows to obtain thin coils with high current density ($\sim 9 \cdot 10^3$ A/cm^2). The colenoids are placed in a vacuum volume formed by flux return yoke (6). The temperature transversal displasmant of the solenoids is prevented by support (11) construction. A dewar (3) of 100 litres liquid helium capacity is situated on the yoke. The helium vapor cooling current leads go through the dewar and were constructed by analogy with Efferson /2/. The maximum working field in the center of the detector is less than the field at the critical current due to degradation current effect in the compensating coils co-working with the main solenoid. The magnetic field inhomogeneity in the working volume is about 15%.

3. Spark and Proportional Chambers

3.1 C o n s t r u c t i o n. The spark chamber and MWPC's design is illustrated in Fig.3. The cylindrical spark chamber's electrodes (3) have been soldered by galium from 0.05 mm aluminium foil. The distance between electrodes is equal to 17.5 mm. The spark chamber has 6 gaps. The inner electrode has 51 mm in diameter and the outer one has 260 mm. The full length of the spark chamber working region is 220 mm. All spark chamber's components have proportions, that no mechanical deformations occur after cooling. The front wall (12), which the volume of the chamber is photographed through, has been made from plexiglass. The rings with prisms (13) that allow the coordinate along the chamber to measure, are attached to the front wall. The stainless steel pipe (9) with 0.05 mm wall thickness is used as a storage ring's vacuum pipe near beams interaction point. To prevent it from outer pressure destruction a beryllium pipe (7) with 1 mm wall thickness is put in. The cathodes of the inner MWPC (8) have been made from gold plated aluminium with 0.15 mm wall thickness. The whole thickness of the vacuum pipe and the electrodes of the MWPC is equal to 0.3 g/cm^2 or 0.009 radiation length. The MWPC have been wound with 28 μ gold plated tungstem wires with 4 mm wire spacing and 2 x 3 mm gap width. All sizes of the MWPC's details from materials with the different heat expansion coefficients were selected to have the constant wires tension with a cooling. The high voltage is led to the sense wires.

3.2 O p t i c a l s y s t e m. The chamber photographs are carried out through the system of mirrors (11) by employment of the camera, that is situated in the focus of the glass spherical lens (10). The lens locates directly in front of the chamber (6) (see Fig.1). The images of two parts of the chamber are taken out from the detector bounds and are brought together on the camera the picture of the whole chamber to have. The coordinates along the chamber are measured with the help of the prisms system that was proposed by S.M.Korenchenko et al. /6/. That system is placed before the front glass of the spark chamber so that part of the spark light hits the camera after going through prisms. Each cylindrical gap has 20 prisms.

3.3 G a s f i l l i n g. One and the same gas mixture is used for the spark chamber and MWPC. The mixture of Ne + 8%Ar + 2.5%CO_2 was found to be suitable at low temperature. The presence of CO_2 in the gas mixture limits the lowest working temperature of the chamber at 170-180 K. With that mixture MWPC's have the plateau width near 100 V with nearly 100% efficiency. The spark chamber memory time in a magnetic field is about 5 sec. The MWPC time resolution is $2\tau \sim 100$ nsec.

3.4 T h e p u l s e h i g h v o l t a g e f e e d i n g of the spark chamber is supplied by means of three Marx generators, that are similar to one described by D.D.Grossmann /3/. Each generator feeds two cylindrical gaps. A generator is built up from 5 steps with 20 kv top voltage on each step. Every generator is situated in a cylindrical box which is filled out with nitrogen at a pressure of 3 atm. The cutting discharger is located inside the box to form back slope of the pulse. Such a generator can produce pulses with amplitudes up to 100 kV and minimal pulse duration of 20 nsec.

3.5 T r i g g e r. Two cylindrical MWPC with sense wires parallel to the beam axes are used for the spark chamber to trigger. The wires in both MWPC are ordered in 16 groups. The signals from every group were taken through a dividing capacitors and proceed via 50Ω cables to the amplifiers, which are outside of the magnet at 5 m distance. The input threshold is adjustable and is normally set at 2 μA. The selection of the desirable coinsidenses is carried out by the block of the trigger logic, which can be changed. The delay time between the particle's passage and the high voltage pulse occuring on the chamber is equal to 300 ÷ 350 nsec.

4. Performance of the Detector

The features of the detector were studied with the cosmic particles. Fig.4 shows some pictures of the cosmic rays tracks. All the pictures were treated with a scanning table and transfered into the computer. Every cosmic particle track going through the center of the detector was treated as two independent tracks. Comparing two parts of the track one can obtain the features of the detector.

4.1 S p a t i a l r e s o l u t i o n. 12 coordinates of the track and 6 coordinates in prisms were measured for each part of the track. A particle trajectory was fitted by a helical curve. The displacements of the sparks in the crossing magnetic field and the electric field of rising slope of high voltage pulse were taken into account. This displacements are about 100 μ . The histograms of mean square displacements of measured track points from the reconstructed helical curve for coordinates in transversal xy plane (σ_R) and for coordinate along the chamber (σ_Z) are shown in Fig.5a,b. An angle resolutions of the detector for two tracks in xy plane (σ_φ) and in perpendicular plane (σ_θ) are shown in Fig.6a,b.

4.2 M o m e n t u m r e s o l u t i o n. Comparing two independently calculated values for two parts of the cosmic particle track one can obtain the momentum resolution of the detector. The results for different momenta are shown in Fig.7. The calculated detector's resolution with $\sigma_R = 55\mu$, the contribution of multiple scattering and relative difference in momentum $\Delta p_{MS}/p_T$ for muons and pions for VEPP-2M energy region are shown in the same picture. In the reactions with two particles in the final state ($e^+e^- \to \mu^+\mu^-, \pi^+\pi^-$) two tracks of the particles with opposite charges can be fitted by one helical curve. In such a case the precision of the momentum fitting depends only on the multiple scattering in the accelerator's vacuum pipe and is equal to σ_p/p = 1.8% for all energies of VEPP-2M (with no radiation corrections taken into account).

4.3 M u l t i t r a c k e f f i c i e n c y of the spark chamber was studied by means of cosmic showers photographs. The results of registration efficiency (ε) measurements for two, three and four particles in one gap are listed in Table 2. There would be two sparks in every gap when the particle goes through the center of the detector, so the gap efficiency with one spark is absent.

Table 2

Number of particle in a gap	2	3	4
ε, %	0.99	0.99	0.95

Only the tracks with angle less than 45° with respect to electric field direction were treated. The listed multitrack efficiency data were obtained with the optimum characters of the high voltage pulse: the amplitude was equal to 90 kV and the pulse duration was 30 ÷ 40 nsec. With such pulse parameters the spark chamber operates close to the streamer mode, so one can see the streamer structure of the spark.

References

1. I.B.Vasserman, I.A.Koop. V.P.Kutovoi et al., Proceedings of the Fifth All-Union Meeting on Charged Particle Accelerators. Moscow, 1976.
2. K.R.Efferson, Rev.Sci.Instr., 1967, 38, N°12, 1776.
3. S.M.Korenchenko, A.G.Morozov, K.G.Nekrasov, U.V.Rodnov. Preprint JINR, R13-5170, Dubna, 1970.
4. D.D.Grossman, Nucl. Instr.Meth., 1967, 51, 165.

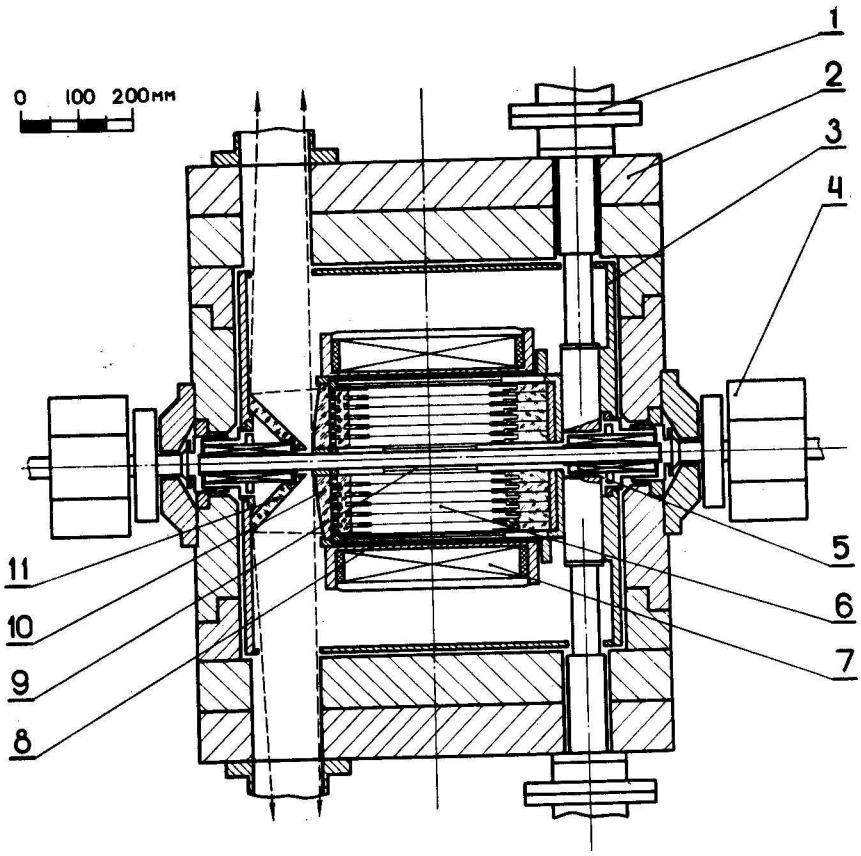

Fig.1. The schematic cross section of the detector. 1 - high voltage feeding, 2 - joke, 3 - nitrogen shell, 4 - magnetic lens of the storage ring, 5 - compensating solenoid, 6 - spark chamber, 7 - main solenoid, 8 - outer MWPC, 9 - inner MWPC, 10 - optic lens, 11 - mirror.

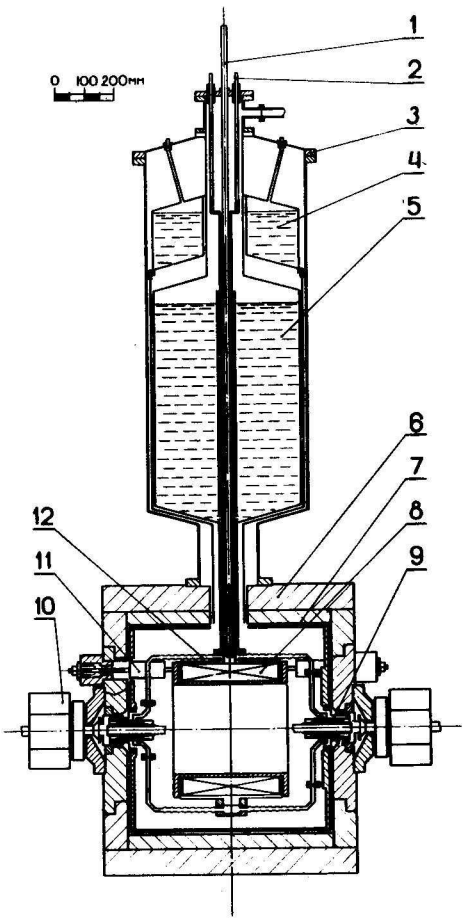

Fig.2 The magnetic system of the detector. 1 - liquid helium supply, 2 - current lead, 3 - dewar, 4 - liquid nitrogen, 5 - liquid helium, 6 - joke, 7 - nitrogen shell, 8 - main solenoid, 9 - compensating solenoid, 10 - magnetic lens, 11 - solenoid support, 12 - helium supply pipe.

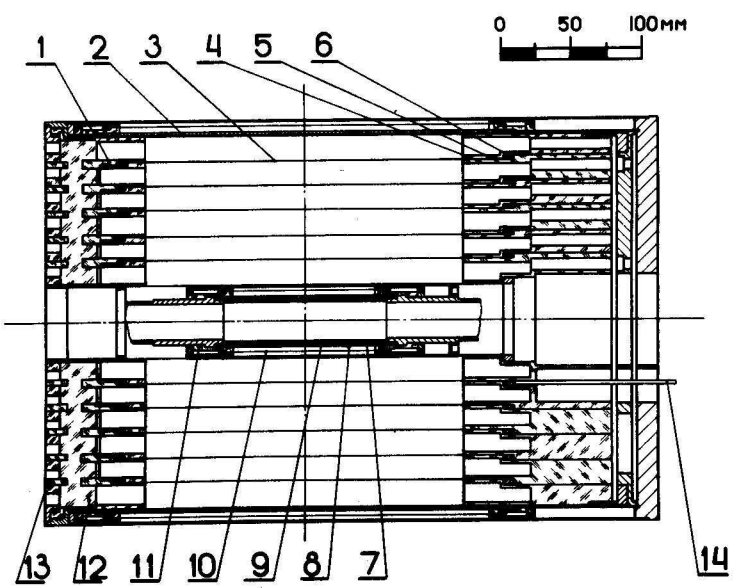

Fig.3 The elements of the spark chamber and MWPC. 1, 4, 5 - isolating rings, 2 - outer electrod of the spark chamber, 3 - foil electrod, 6 - aluminium ring, 7 - berillium pipe, 8 - MWPC electrod, 9 - vacuum pipe, 10 - sense wire, 11 - isolating ring, 12 - front wall, 13 - prisms, 14 - supply electrod.

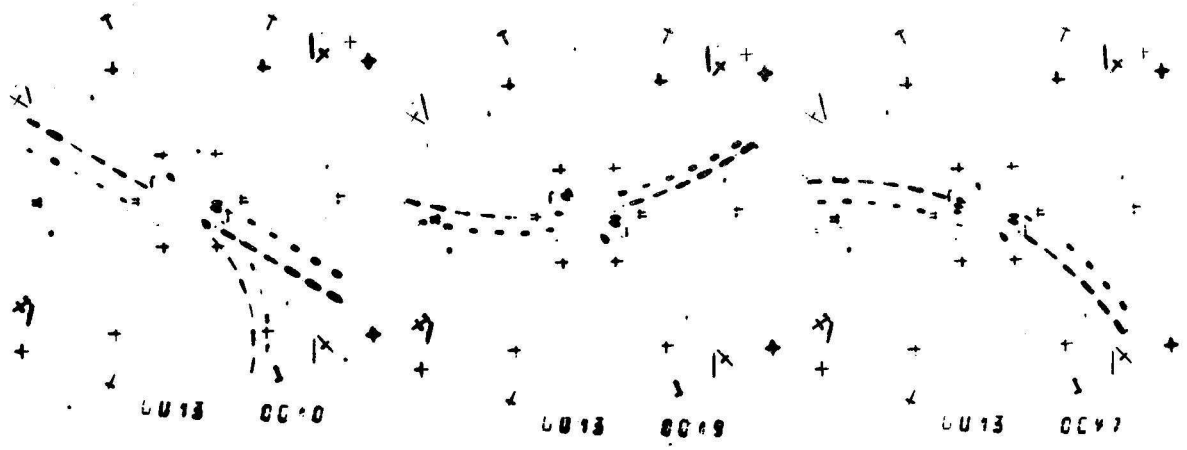

Fig.4 The pictures of the cosmic events

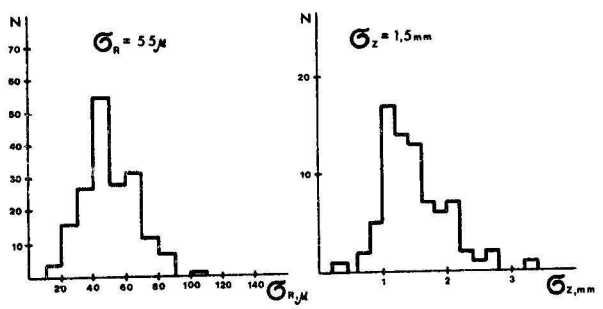

Fig.5 The spatial resolution of the detector in xy plane (a) and in perpendicular plane (b)

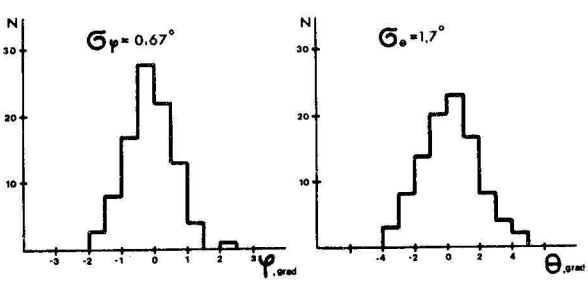

Fig.6 The angle resolution of the detector for two particles in xy plane (a) and in perpendicular plane (b)

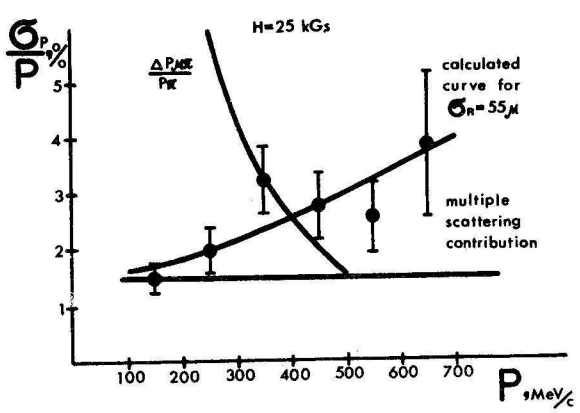

Fig.7 The momentum resolution of the detector

Работа поступила - 4 октября 1976 г.

Ответственный за выпуск - С.Г.ПОПОВ
Подписано к печати - 10.XII-1976г. МН 03057
Усл. 1,3 печ.л., 1,1 учетно-изд.л.
Тираж 200 экз. Бесплатно
Заказ № 121.

Отпечатано на ротапринте ИЯФ СО АН СССР